

## (*E*)-4-[2-(3,4,5-Trimethoxyphenyl)-ethenyl]nitrobenzene and its 'bridge-flipped' analogues

Alain Collas and Frank Blockhuys\*

Department of Chemistry, University of Antwerp, Universiteitsplein 1, B-2610 Antwerp, Belgium

Correspondence e-mail: frank.blockhuys@ua.ac.be

Received 5 July 2011

Accepted 1 August 2011

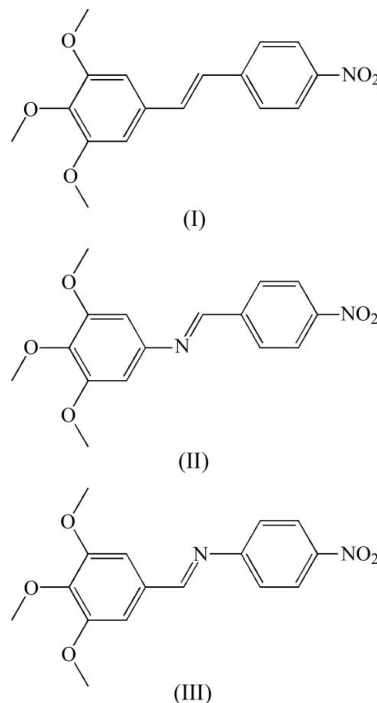
Online 17 August 2011

The solid-state structures of three push–pull acceptor– $\pi$ -donor ( $A$ - $\pi$ - $D$ ) systems differing only in the nature of the  $\pi$ -spacer have been determined. (*E*)-1-Nitro-4-[2-(3,4,5-trimethoxyphenyl)ethenyl]benzene,  $C_{17}H_{17}NO_5$ , (I), and its 'bridge-flipped' imine analogues, (*E*)-3,4,5-trimethoxy-*N*-(4-nitrobenzylidene)aniline,  $C_{16}H_{16}N_2O_5$ , (II), and (*E*)-4-nitro-*N*-(3,4,5-trimethoxybenzylidene)aniline,  $C_{16}H_{16}N_2O_5$ , (III), display different kinds of supramolecular networks, *viz.* corrugated planes, a herringbone pattern and a layered structure, respectively, all with zero overall dipole moments. Only (III) crystallizes in a noncentrosymmetric space group ( $P2_12_12_1$ ) and is, therefore, a potential material for second-harmonic generation (SHG).

### Comment

For several years now, the liquid-crystal-forming properties of *N*-benzylideneaniline (BA) and its derivatives have been studied in great detail (Kitamura *et al.*, 1986; Ajeetha & Pisipati, 2006; Fakruddin *et al.*, 2009); their rod-like shape is the basis of a number of unique properties which lead to calamitic liquid crystals that may find application in customizable electro-optical switches. The aromatic moieties in BAs have been described as the main recognition points of the mesogens used in the organization of the liquid-crystalline superstructure (Neuvonen *et al.*, 2006). Extended alkyl or alkoxy chains are substituted onto these aromatic fragments to introduce the necessary flexibility into the molecular structure, and this flexibility is further enhanced by the imine spacers present in the BA. It is the subtle equilibrium between the rigid rod-like structure and the presence of flexible groups that determines the physical properties of the liquid-crystalline phase. Since the solid-state structures of these materials can not be studied in the liquid-crystalline phase, the extended side chains must be replaced by shorter ones, such as methoxy groups, in order to investigate the intermolecular interactions involving the mesogen.

Push–pull acceptor– $\pi$ -donor ( $A$ - $\pi$ - $D$ ) systems are of particular interest in this context because of their superior charge-transfer-related nonlinear electrical and optical properties, such as the electro-optic effect (EO) and second-harmonic generation (SHG). Unfortunately, the large molecular dipoles associated with such push–pull systems usually lead to centrosymmetric organization of the molecules in the crystal structure, annihilating bulk second-order optical effects such as SHG. It has been suggested that whether or not an asymmetric dipolar BA crystallizes centrosymmetrically is largely dependent on the molecular planarity, which may be directly



related to the molecular rigidity mentioned above; more planar molecules have a greater possibility of crystallizing in a noncentrosymmetric space group (Zhang, 2002). To verify Zhang's correlation, a search of the Cambridge Structural Database (CSD, Version 5.32, with update of February 2011; Allen, 2002) was conducted for all stilbenes and BAs having no *ortho* substituents. Indeed, since *ortho* substituents can easily give rise to steric hindrance or intramolecular hydrogen bonding, a correlation involving the planarity of the systems would be biased. Erroneous, cocrystal, polymeric, ionic, powder and organometallic structures, and symmetric structures with  $Z' = 0.5$ , were also excluded. On the other hand, heterocyclic rings with the heteroatom in the 3-, 4- or 5-position were allowed. For the stilbenes, only *E* configurations [ $\tau(C1-C7-C8-C9) = 180 \pm 15^\circ$ ] were considered. The distribution of torsion angles in the resulting structures is given in Fig. 1. As can be seen from these polar histograms, the stilbenes are all quasiplanar (Fig. 1*a*). The majority of the BAs, on the other hand, display conformations with torsion angles within the  $\pm 45^\circ$  range (Fig. 1*b*). 64 of the 169 stilbenes and 44 of the 178 BAs found belong to noncentrosymmetric space groups. 53 stilbenes and 81 BAs are donor–acceptor (*DA*) systems. 17 and 19 of these, respectively, belong to noncen-

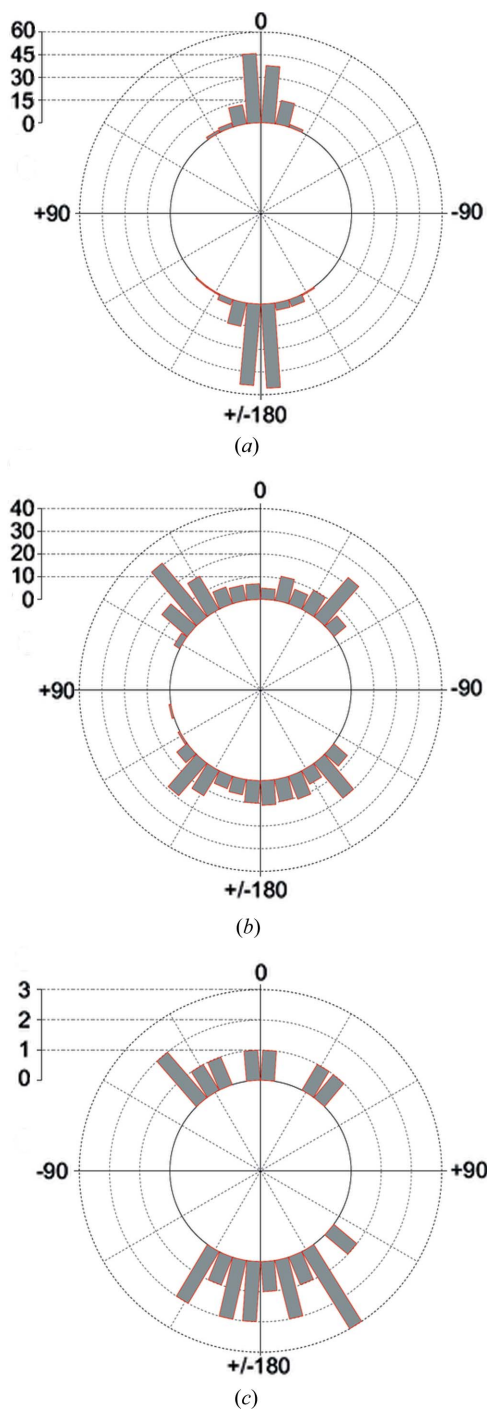


**Figure 1**

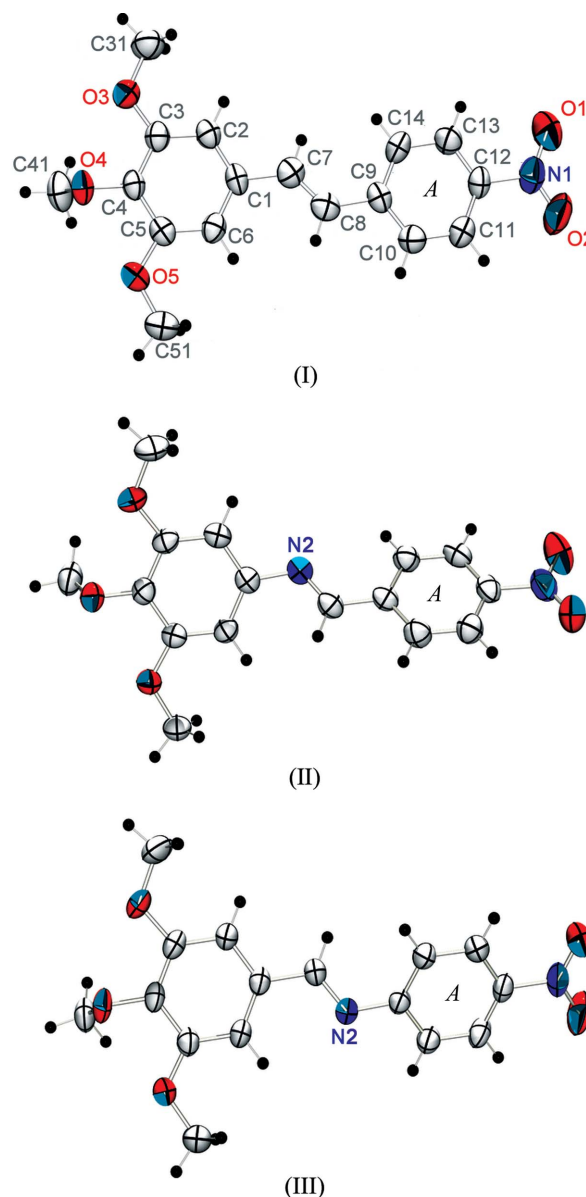
Polar histograms illustrating the distribution of (a) torsion angles  $\tau(\text{C2}-\text{C1}-\text{C7}-\text{C8})$  in stilbenes, (b) torsion angles  $\tau(\text{C2}-\text{C1}-\text{N2}-\text{C8})$  in BAs and (c) torsion angles of donor-acceptor BAs in noncentrosymmetric space groups; see *Comment* for details.

trosymmetric space groups. As can be seen from Fig. 1(c) though, the torsion angles of these 19 BAs (or 23 structures, with the addition of four polymorphs) are quite well distributed over the entire  $\pm 45^\circ$  range. Based on these results, the suggested correlation seems unlikely.

It is interesting to note that usually just one of the structures of the three possible stilbene/BA derivatives (*i.e.* with  $-\text{CH}=\text{CH}-$ ,  $-\text{CH}=\text{N}-$  or  $-\text{N}=\text{CH}-$  as spacer) is

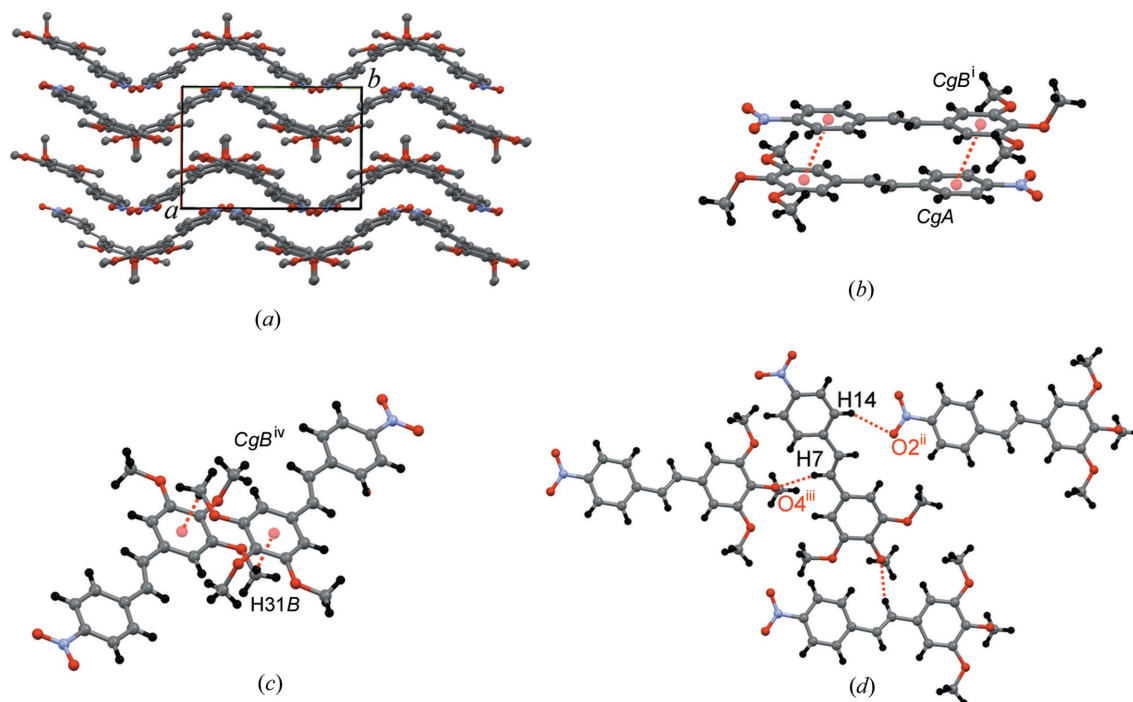
available, so that a direct comparison of the effect of the spacer on the supramolecular structure is impossible. In order to make just such a comparison, the stilbene (*E*)-1-nitro-4-[2-(3,4,5-trimethoxyphenyl)ethenyl]benzene, (I), and its two 'bridge-flipped' (Ojala *et al.*, 2009) imine derivatives, (*E*)-3,4,5-trimethoxy-*N*-(4-nitrobenzylidene)aniline, (II), and (*E*)-4-nitro-*N*-(3,4,5-trimethoxybenzylidene)aniline, (III) (Fig. 2), were prepared and structurally characterized.

Compounds (I) and (II) crystallize in the centrosymmetric space group  $P2_1/c$ , while (III) crystallizes in the chiral space group  $P2_12_12_1$ . Compound (I) is quasipolar, while the imine derivatives (II) and (III) display the typical  $40^\circ$  twist around the C–N bond which is also found in the calculated gas-phase



**Figure 2**

The molecular structures of (I), (II) and (III), showing the atom-numbering scheme. In each case, the nitro-substituted ring is labelled A. Displacement ellipsoids are drawn at the 50% probability level. H atoms are represented by spheres of arbitrary radii and bear the same number as the C atom to which they are attached.

**Figure 3**

(a) The corrugated planes in the structure of (I), held together by (b)  $\pi$ - $\pi$ , (c)  $\text{OCH}_3 \cdots \pi$  and (d)  $\text{C}-\text{H} \cdots \text{O}$  interactions (all interactions are shown as dashed lines). Symmetry codes are as in Table 2.

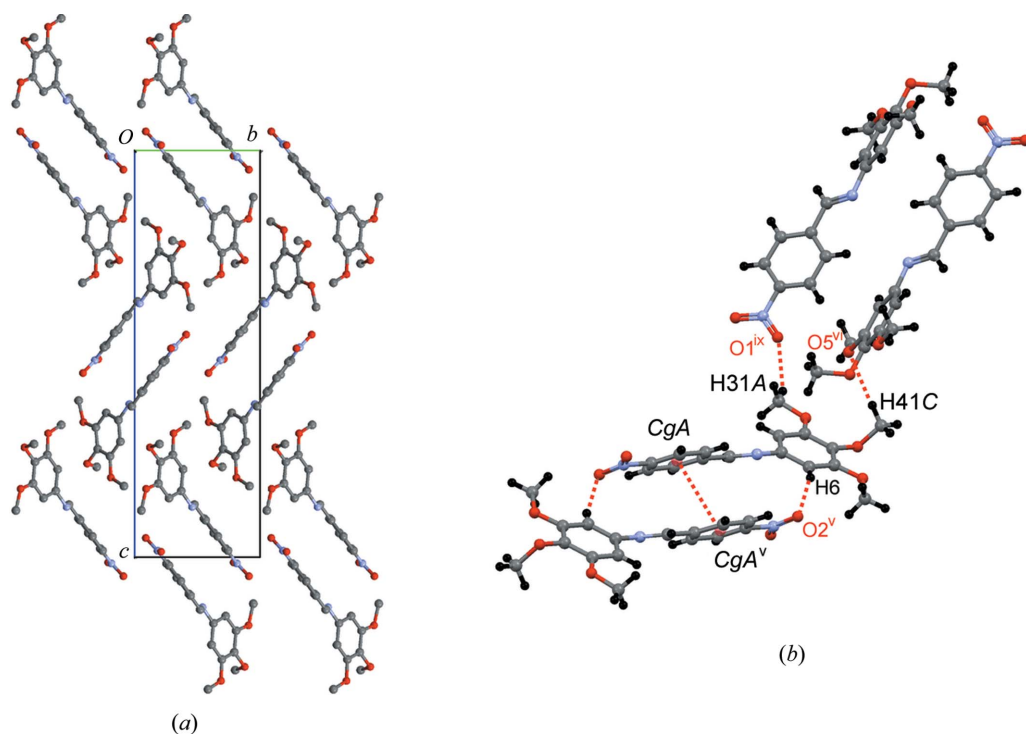
structures, as evidenced by the values of  $\tau(\text{C1}-\text{N2})$  for (II) and  $\tau(\text{N2}-\text{C9})$  for (III) in Table 1.

The quasiplanar molecules of (I) (Fig. 3a) form pairs, in which the two molecules are held together by dipolar forces and  $\pi^{\delta+}-\pi^{\delta-}$  interactions, with  $\text{CgA} \cdots \text{CgB}^i = 3.936(4) \text{ \AA}$  [ $\text{CgA}$  and  $\text{CgB}$  are the centroids of the nitro-substituted (A) and trimethoxy-substituted (B) benzene rings, respectively; symmetry code: (i)  $-x, -y + 1, -z$ ],  $\alpha = 2.20(14)^\circ$  and  $\gamma = 30.07^\circ$ , where  $\alpha$  is defined as the dihedral angle between the least-squares (LS) planes through rings A and B, and  $\gamma$  as the angle between the  $\text{CgA} \cdots \text{CgB}$  vector and the normal to the LS plane through ring B (Fig. 3b). This two-by-two arrangement leads to layers in which the distance between the molecules is less than  $4.2 \text{ \AA}$  – the photochemical criterion (Schmidt, 1971) – and, as a consequence, this crystal structure should be photosensitive, but this was not observed during the manipulation of the compound. These nonpolar pairs are further stabilized on both sides by weak hydrogen bonds involving the O atom of the nitro group (Fig. 3d and entry 1 in Table 2) and an O atom of a methoxy group (Fig. 3d and entry 2 in Table 2), which gives a structure formed of planes two molecules thick. These planes are then fused together by reciprocal  $\text{OCH}_3 \cdots \pi$  contacts (Fig. 3c and entry 3 in Table 2). The overall result is a supramolecular structure of corrugated planes (Fig. 3a).

The crystal structure of (II) is also based on pairs of molecules in which their large individual dipoles are cancelled. As a result,  $\pi$ - $\pi$  stacking can be easily recognized [ $\text{CgA} \cdots \text{CgA}^v = 3.993(1) \text{ \AA}$ ,  $\alpha = 0.0^\circ$  and  $\gamma = 25.79^\circ$ ; symmetry code: (v)  $-x + 1, -y + 2, -z + 1$ ] (Fig. 4). These dimers are further stabilized by

a mutual weak hydrogen bond involving atom H6 and an O atom of the nitro group (Fig. 4b and entry 1 in Table 3). Ribbons are then generated by a weak  $\text{C}-\text{H} \cdots \text{O}$  hydrogen bond between the methoxy groups in the 4- and 5-positions (Fig. 4b and entry 2 in Table 3). Simultaneously, atom H41B engages in a  $\text{C}-\text{H} \cdots \pi$  contact with the  $\pi$ -system of the methoxy-substituted aniline fragment (entry 3 in Table 3, not shown in Fig. 4). Perpendicular to these ribbons, another  $\text{OCH}_3 \cdots \pi$  contact is initiated by the methoxy group in the 3-position, which is made possible by the twist of the aniline ring (entry 4 in Table 3, not shown in Fig. 4). In the third direction, a  $\text{C}-\text{H} \cdots \text{O}$  interaction (entry 5 in Table 3) and an  $\text{OCH}_3 \cdots \pi$  interaction (entry 6 in Table 3) stabilize the structure further (not shown in Fig. 4). Both the imine N atom and the relatively acidic H8 atom remain unused in this structure.

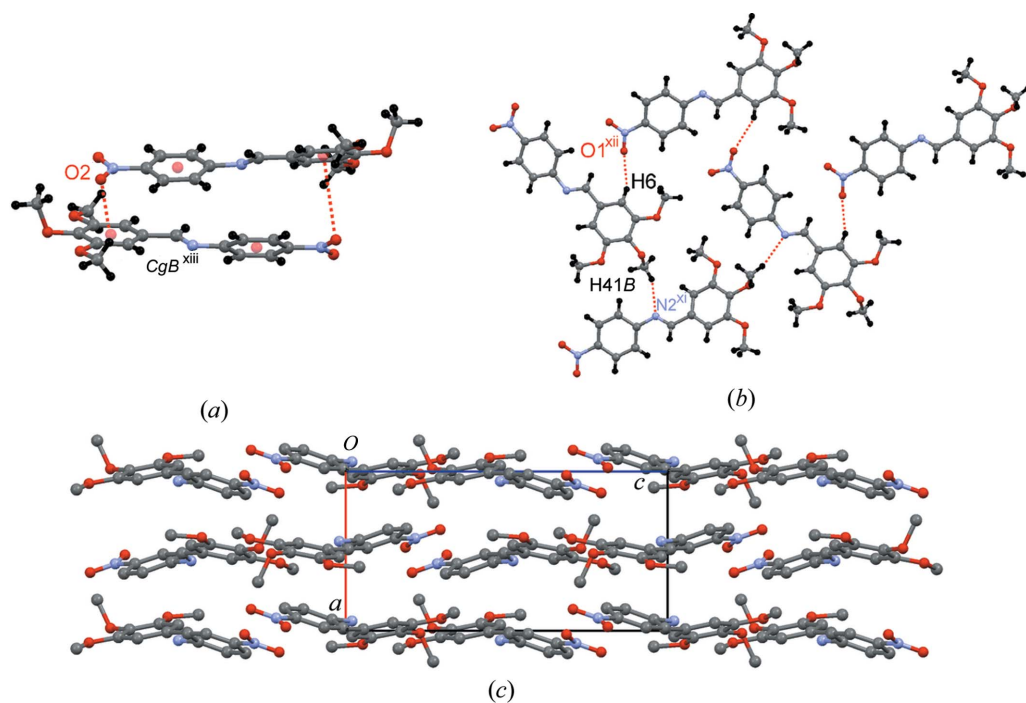
Compound (III), which crystallizes in the chiral space group  $P2_12_12_1$ , does not form these antiparallel assemblies. It is remarkable that a hydrogen bond involving imine atom N2 as acceptor generates a ribbon of molecules in the  $bc$  plane (Fig. 5b and entry 1 in Table 4). These ribbons are further expanded into a plane of molecules by an additional hydrogen bond (Fig. 5b and entry 2 in Table 4). In the direction perpendicular to the plane, the [100] direction, atom O2 of the nitro group contacts the  $\pi$ -systems of the aniline rings in the planes above (Fig. 5a and entry 3 in Table 4) and below the molecule (entry 4 in Table 4, not shown in Fig. 5). Thus, the layered structure (Fig. 5c) is stabilized in all three directions, but as a result of this particular stacking, the molecular dipoles add up to zero, in keeping with the observed space group symmetry.

**Figure 4**

(a) The herringbone pattern in the structure of (II), viewed along the  $a$  axis and (b) the various other intermolecular contacts (dashed lines). Symmetry codes are as in Table 3.

It may be clear from the above that (I) and (II) aggregate as dimers, cancelling out the net dipole in each case and constructing centrosymmetric corrugated layered and herringbone networks, respectively.  $\pi$ - $\pi$  stacking involving the

nitro-substituted  $A$  rings occurs in the solid-state structures of (I) and (II) as a consequence of the contribution of dipolar forces (see Table 1 for the calculated dipole moments). The methoxy groups are engaged in almost equal numbers of

**Figure 5**

(a) The  $\text{NO} \cdots \pi$  contacts, (b) the interactions within the layers and (c) the layered structure of (III), viewed along  $b$  (all interactions are shown as dashed lines). Symmetry codes are as in Table 4.

OCH<sub>3</sub>···π and C—H···O interactions. Surprisingly, compound (III) possesses the largest dipole but displays a noncentrosymmetric network based on weak hydrogen bonds involving the imine N atom. The chiral network is essential for displaying nonlinear responses based on the second-order nonlinear electrical susceptibility ( $\chi^{(2)}$ ).

### Experimental

All reagents and solvents were obtained from ACROS and used as received. All NMR spectra were recorded on a Bruker Avance II spectrometer at frequencies of 400 MHz for <sup>1</sup>H and 100 MHz for <sup>13</sup>C in CDCl<sub>3</sub> with tetramethylsilane (TMS) as internal standard; chemical shifts  $\delta$  are given in p.p.m. and coupling constants  $J$  in Hz. Melting points were obtained with an open capillary electrothermal melting-point apparatus and are uncorrected.

(*E*)-1-Nitro-4-[2-(3,4,5-trimethoxyphenyl)ethenyl]benzene, (I), was prepared by adding LiOH (0.7 g, 0.03 mol) to a stirred solution of (4-nitrobenzyl)triphenylphosphonium chloride (13.1 g, 0.03 mol) and 3,4,5-trimethoxybenzaldehyde (6.0 g, 0.03 mol) in propan-2-ol (110 ml). The resulting suspension was refluxed for 18 h. After cooling to room temperature, water (100 ml) was added, and since no precipitate was formed the solution was extracted with diethyl ether (3 × 50 ml). The organic layer was separated off and evaporated to dryness. Isomerization of the crude product in *p*-xylene (50 ml) with a catalytic amount of I<sub>2</sub> yielded 2.4 g (0.007 mol, 23%) of long yellow needles of (I). Characterization: m.p. 466 K; <sup>1</sup>H NMR:  $\delta$  3.89 (*s*, 3H, 4-OCH<sub>3</sub>), 3.93 (*s*, 6H, 3-OCH<sub>3</sub> and 5-OCH<sub>3</sub>), 6.78 (*s*, 2H, H2 and H6), 7.03 (*d*, <sup>3</sup> $J$  = 16.1, 1H, H7), 7.19 (*d*, <sup>3</sup> $J$  = 16.1, 1H, H8), 7.61 (*d*, <sup>3</sup> $J$  = 8.2, 2H, H11 and H13), 8.20 (*d*, <sup>3</sup> $J$  = 8.2, 2H, H10 and H14); <sup>13</sup>C NMR:  $\delta$  56.22 (3-OCH<sub>3</sub> and 5-OCH<sub>3</sub>), 60.98 (4-OCH<sub>3</sub>), 104.32 (C2 and C6), 124.15 (C10 and C14), 125.69 (C8), 126.74 (C7), 131.86 (C11 and C13), 133.31 (C1), 139.13 (C4), 143.82 (C12), 146.73 (C9), 153.56 (C3 and C5). Crystals used in the diffraction experiment were grown by slow cooling of an ethyl acetate–hexane (1:1 *v/v*) solution.

(*E*)-3,4,5-Trimethoxy-*N*-(4-nitrobenzylidene)aniline, (II), was prepared by dissolving 3,4,5-trimethoxyaniline (1.8 g, 0.01 mol) and 4-nitrobenzaldehyde (1.5 g, 0.01 mol) in ethanol (100 ml) and stirring the solution overnight. The orange precipitate which formed was filtered off, yielding 3.0 g (9.5 mmol, 95%) of (II). Characterization: m.p. 430 K; <sup>1</sup>H NMR:  $\delta$  3.88 (*s*, 3H, 4-OCH<sub>3</sub>), 3.92 (*s*, 6H, 3-OCH<sub>3</sub> and 5-OCH<sub>3</sub>), 6.56 (*s*, 2H, H2 and H6), 8.07 (*d*, <sup>3</sup> $J$  = 8.8, 2H, H10 and H14), 8.32 (*d*, <sup>3</sup> $J$  = 8.8, 2H, H11 and H13), 8.57 (*s*, 1H, H8); <sup>13</sup>C NMR:  $\delta$  56.23 (3-OCH<sub>3</sub> and 5-OCH<sub>3</sub>), 61.02 (4-OCH<sub>3</sub>), 98.60 (C2 and C6), 124.03 (C11 and C13), 129.31 (C10 and C14), 137.58 (C4), 141.53 (C9), 146.63 (C1), 149.31 (C12), 153.86 (C3 and C5), 156.40 (C8). Crystals used in the diffraction experiment were grown by slow evaporation from a CH<sub>2</sub>Cl<sub>2</sub> solution.

(*E*)-4-Nitro-*N*-(3,4,5-trimethoxybenzylidene)aniline, (III), was prepared by refluxing 3,4,5-trimethoxybenzaldehyde (3.0 g, 0.015 mol) and 4-nitroaniline (2.1 g, 0.015 mol) in methanol (100 ml) for 3 h. The resulting yellow precipitate was collected by filtration and recrystallized from acetonitrile, yielding 3.5 g (11 mmol, 75%) of (III). Crystals from this batch were used in the crystallographic experiment. Characterization: m.p. 428 K; <sup>1</sup>H NMR:  $\delta$  3.94 (*s*, 3H, 4-OCH<sub>3</sub>), 3.95 (*s*, 6H, 3-OCH<sub>3</sub> and 5-OCH<sub>3</sub>), 7.18 (*s*, 2H, H2 and H6), 7.23 (*dd*, <sup>3</sup> $J$  = 8.9, <sup>4</sup> $J$  = 1.9, 2H, H10 and H14), 8.25 (*dd*, <sup>3</sup> $J$  = 8.9, <sup>4</sup> $J$  = 1.9, 2H, H11 and H13), 8.32 (*s*, 1H, H7); <sup>13</sup>C NMR:  $\delta$  56.33 (3-OCH<sub>3</sub> and 5-OCH<sub>3</sub>), 61.03 (4-OCH<sub>3</sub>), 106.44 (C2 and C6), 121.29 (C10 and C14), 125.04 (C11 and C13), 130.81 (C1), 142.01 (C4), 145.45 (C12), 153.65 (C3 and C5), 157.87 (C9), 162.08 (C7).

### Compound (I)

#### Crystal data

C<sub>17</sub>H<sub>17</sub>NO<sub>5</sub>  
*M<sub>r</sub>* = 315.32  
 Monoclinic, *P*2<sub>1</sub>/*c*  
*a* = 10.459 (2) Å  
*b* = 12.88 (1) Å  
*c* = 14.021 (4) Å  
 $\beta$  = 124.069 (15)°

*V* = 1564.6 (13) Å<sup>3</sup>  
*Z* = 4  
 Mo *K*α radiation  
 $\mu$  = 0.10 mm<sup>-1</sup>  
*T* = 293 K  
 0.42 × 0.39 × 0.39 mm

#### Data collection

Enraf–Nonius CAD-4  
 diffractometer  
 5901 measured reflections  
 2867 independent reflections

1500 reflections with *I* > 2σ(*I*)  
*R*<sub>int</sub> = 0.043  
 3 standard reflections every 60 min  
 intensity decay: none

#### Refinement

*R*[*F*<sup>2</sup> > 2σ(*F*<sup>2</sup>)] = 0.045  
*wR*(*F*<sup>2</sup>) = 0.135  
*S* = 1.00  
 2867 reflections

211 parameters  
 H-atom parameters constrained  
 $\Delta\rho_{\max}$  = 0.35 e Å<sup>-3</sup>  
 $\Delta\rho_{\min}$  = -0.14 e Å<sup>-3</sup>

### Compound (II)

#### Crystal data

C<sub>16</sub>H<sub>16</sub>N<sub>2</sub>O<sub>5</sub>  
*M<sub>r</sub>* = 316.31  
 Monoclinic, *P*2<sub>1</sub>/*c*  
*a* = 7.512 (2) Å  
*b* = 7.895 (1) Å  
*c* = 26.441 (6) Å  
 $\beta$  = 104.667 (19)°

*V* = 1517.0 (6) Å<sup>3</sup>  
*Z* = 4  
 Mo *K*α radiation  
 $\mu$  = 0.10 mm<sup>-1</sup>  
*T* = 293 K  
 0.3 × 0.3 × 0.3 mm

#### Data collection

Enraf–Nonius CAD-4  
 diffractometer  
 5826 measured reflections  
 2803 independent reflections

2023 reflections with *I* > 2σ(*I*)  
*R*<sub>int</sub> = 0.052  
 3 standard reflections every 60 min  
 intensity decay: 4%

**Table 1**

Selected geometric data for (I), (II) and (III); calculated (DFT) and experimental (XRD) torsion angles in degrees (°), and calculated dipole moments  $\mu$  in Debye.

Compound	Parameter	XRD	DFT	$\mu$
(I)	C2–C1–C7–C8	–11.0 (5)	176.2	5.48
	C1–C7–C8–C9	178.7 (3)	0.3	
	C7–C8–C9–C10	–172.1 (3)	4.2	
(II)	C2–C1–N2–C8	–38.4 (2)	31.6	4.59
	C1–N2–C8–C9	179.4 (1)	177.4	
(III)	N2–C8–C9–C10	–11.5 (2)	1.4	6.15
	C2–C1–C7–N2	4.1 (4)	1.4	
	C1–C7–N2–C9	177.8 (2)	176.4	
	C7–N2–C9–C10	–39.5 (4)	42.5	

**Table 2**

Weak hydrogen bonds in (I) (Å, °).

Entry	<i>D</i>	H	<i>A</i>	H··· <i>A</i>	<i>D</i> ··· <i>A</i>	<i>D</i> –H··· <i>A</i>
1	C14	H14	O2 <sup>ii</sup>	2.69	3.526 (4)	151
2	C7	H7	O4 <sup>iii</sup>	2.57	3.447 (3)	158
3	C31	H31 <i>B</i>	C <i>gB</i> <sup>iv</sup>	2.83	3.718 (5)	154

Symmetry codes: (ii) *x*, –*y* +  $\frac{1}{2}$ , *z* –  $\frac{1}{2}$ ; (iii) *x*, –*y* +  $\frac{3}{2}$ , *z* +  $\frac{1}{2}$ ; (iv) *x* + 1, –*y* + 1, –*z*.

**Table 3**  
Weak hydrogen bonds in (II) (Å, °).

Entry	D	H	A	H...A	D...A	D—H...A
1	C6	H6	O2 <sup>v</sup>	2.54	3.423 (2)	160
2	C41	H41C	O5 <sup>vi</sup>	2.50	3.450 (3)	168
3	C41	H41B	CgB <sup>viii</sup>	2.96	3.626 (3)	128
4	C31	H31A	CgB <sup>viii</sup>	2.78	3.463 (3)	129
5	C31	H31B	O1 <sup>ix</sup>	2.71	3.542 (3)	145
6	C51	H51B	CgA <sup>x</sup>	2.94	3.631 (3)	130

Symmetry codes: (v)  $-x + 1, -y + 2, -z + 1$ ; (vi)  $-x + 3, y + \frac{1}{2}, -z + \frac{3}{2}$ ; (vii)  $-x + 3, y - \frac{1}{2}, -z + \frac{3}{2}$ ; (viii)  $-x + 2, y + \frac{1}{2}, -z + \frac{3}{2}$ ; (ix)  $x + 1, -y + \frac{3}{2}, z + \frac{1}{2}$ ; (x)  $x + 1, y - 1, z$ .

**Table 4**  
Short contacts in (III) (Å, °).

Entry	D	X	A	X...A	D...A	D—X...A
1	C41	H41B	N2 <sup>xi</sup>	2.66	3.537 (4)	153
2	C6	H6	O1 <sup>xii</sup>	2.58	3.450 (4)	156
3	N1	O2	CgB <sup>xiii</sup>	3.610 (4)	3.587 (4)	79.1 (2)
4	N1	O2	CgB <sup>xiv</sup>	3.912 (4)	4.578 (4)	115.7 (2)

Symmetry codes: (xi)  $-x, \frac{1}{2} + y, \frac{1}{2} - z$ ; (xii)  $-x, \frac{1}{2} + y, -\frac{1}{2} - z$ ; (xiii)  $-\frac{1}{2} + x, \frac{1}{2} - y, -z$ ; (xiv)  $\frac{1}{2} + x, \frac{1}{2} - y, -z$ .

**Refinement**

$R[F^2 > 2\sigma(F^2)] = 0.036$  211 parameters  
 $wR(F^2) = 0.104$  H-atom parameters constrained  
 $S = 1.05$   $\Delta\rho_{\max} = 0.14 \text{ e } \text{Å}^{-3}$   
 2803 reflections  $\Delta\rho_{\min} = -0.18 \text{ e } \text{Å}^{-3}$

**Compound (III)****Crystal data**

C<sub>16</sub>H<sub>16</sub>N<sub>2</sub>O<sub>5</sub>  $V = 1519.4 (8) \text{ Å}^3$   
 $M_r = 316.31$   $Z = 4$   
 Orthorhombic,  $P2_12_12_1$  Mo  $K\alpha$  radiation  
 $a = 7.215 (3) \text{ Å}$   $\mu = 0.10 \text{ mm}^{-1}$   
 $b = 14.429 (2) \text{ Å}$   $T = 293 \text{ K}$   
 $c = 14.595 (5) \text{ Å}$   $0.4 \times 0.4 \times 0.3 \text{ mm}$

**Data collection**

Enraf–Nonius CAD-4 1358 reflections with  $I > 2\sigma(I)$   
 diffractometer  $R_{\text{int}} = 0.057$   
 4683 measured reflections 3 standard reflections every 60 min  
 1618 independent reflections intensity decay: 10%

**Refinement**

$R[F^2 > 2\sigma(F^2)] = 0.052$  212 parameters  
 $wR(F^2) = 0.141$  H-atom parameters constrained  
 $S = 1.07$   $\Delta\rho_{\max} = 0.30 \text{ e } \text{Å}^{-3}$   
 1618 reflections  $\Delta\rho_{\min} = -0.21 \text{ e } \text{Å}^{-3}$

The molecular structures of isolated molecules of (I), (II) and (III) were optimized at the DFT/B3LYP/6-31G\* level of theory using the GAUSSIAN09 program package (Frisch *et al.*, 2009); the functional and basis set were used as they are implemented in the program. Frequency calculations were performed to ascertain that the resulting structures are minima on the potential-energy surface (PES). Molecular dipoles of the four molecules in the unit cell of (III) were calculated in their solid-state geometries at the same level of theory. The resulting vectors were then transformed from the Cartesian to

the unit-cell coordinate system. The polar histograms were generated using the VISTA program in the CSD suite.

All H atoms were treated as riding using SHELXL97 (Sheldrick, 2008) defaults at 293 (1) K, with C—H = 0.93 Å and  $U_{\text{iso}}(\text{H}) = 1.2U_{\text{eq}}(\text{C})$  for aromatic H atoms, and C—H = 0.96 Å and  $U_{\text{iso}}(\text{H}) = 1.5U_{\text{eq}}(\text{C})$  for methyl H atoms. The displacement parameters of atoms C7 and C8 in (I) seem to suggest disorder typical of ethenyl spacers in stilbene-type systems (see Vande Velde *et al.*, 2011), but attempts to refine a disordered model did not lead to satisfactory results. However, since only a small fraction of misoriented fragments is present, the quality of the nondisordered model was found to be sufficient, even though this leads to slightly larger displacement ellipsoids for the mentioned atoms. For (III), Friedel pairs were collected independently but were merged (MERG 3 command in SHELXL97) for the final refinement. In the absence of a heavy atom [ $Z > 14$  (Si)], and with the use of Mo radiation, anomalous scattering could not be used to determine an absolute structure and thus it was chosen arbitrarily.

For all compounds, data collection: CAD-4 EXPRESS (Enraf–Nonius, 1994); cell refinement: CAD-4 EXPRESS; data reduction: XCAD4 (Harms & Wocadlo, 1996); program(s) used to solve structure: SHELXS97 (Sheldrick, 2008); program(s) used to refine structure: SHELXL97 (Sheldrick, 2008); molecular graphics: ORTEP-3 (Farrugia, 1997) and Mercury (Macrae *et al.*, 2008); software used to prepare material for publication: WinGX (Farrugia, 1999) and PLATON (Spek, 2009).

AC thanks the Institute for the Promotion of Innovation by Science and Technology in Flanders (IWT) for his predoctoral grants. Financial support by FWO–Vlaanderen under grant No. G.0129.05 and by the University of Antwerp under grant No. GOA-2404 is gratefully acknowledged.

Supplementary data for this paper are available from the IUCr electronic archives (Reference: FA3256). Services for accessing these data are described at the back of the journal.

**References**

- Ajeetha, N. & Pisipati, V. G. K. M. (2006). *Mol. Cryst. Liq. Cryst.* **457**, 3–25.  
 Allen, F. H. (2002). *Acta Cryst.* **B58**, 380–388.  
 Enraf–Nonius (1994). CAD-4 EXPRESS. Enraf–Nonius, Delft, The Netherlands.  
 Fakruddin, K., Kumar, R. J., Prasad, P. V. D. & Pisipati, V. G. K. M. (2009). *Mol. Cryst. Liq. Cryst.* **511**, 1616–1627.  
 Farrugia, L. J. (1997). *J. Appl. Cryst.* **30**, 565.  
 Farrugia, L. J. (1999). *J. Appl. Cryst.* **32**, 837–838.  
 Frisch, M. J., *et al.* (2009). GAUSSIAN09. Revision A.02. Gaussian Inc., Pittsburgh, Pennsylvania, USA.  
 Harms, K. & Wocadlo, S. (1996). XCAD4. University of Marburg, Germany.  
 Kitamura, T., Mukoh, A., Isogai, M., Inukai, T., Furukawa, K. & Terashima, K. (1986). *Mol. Cryst. Liq. Cryst.* **136**, 167–173.  
 Macrae, C. F., Bruno, I. J., Chisholm, J. A., Edgington, P. R., McCabe, P., Pidcock, E., Rodriguez-Monge, L., Taylor, R., van de Streek, J. & Wood, P. A. (2008). *J. Appl. Cryst.* **41**, 466–470.  
 Neuvonen, H., Neuvonen, K. & Fulop, F. (2006). *J. Org. Chem.* **71**, 3141–3148.  
 Ojala, W. H., Lystad, K. M., Deal, T. L., Engelbretson, J. E., Spude, J. M., Balidemaj, B. & Ojala, C. R. (2009). *Cryst. Growth Des.* **9**, 964–970.  
 Schmidt, G. M. J. (1971). *Pure Appl. Chem.* **27**, 647–678.  
 Sheldrick, G. M. (2008). *Acta Cryst.* **A64**, 112–122.  
 Spek, A. L. (2009). *Acta Cryst.* **D65**, 148–155.  
 Vande Velde, C. M. L., Collas, A., De Borger, R. & Blockhuys, F. (2011). *Chem. Eur. J.* **17**, 912–919.  
 Zhang, D.-C. (2002). *Acta Cryst.* **C58**, o351–o352.